Journal of Dermatological Science 94 (2019) 205–212

Contents lists available at ScienceDirect

Journal of Dermatological Science

journal homepage: www.jdsjournal.com

Original artcle

COA-Cl prevented TGF-β1-induced CTGF expression by Akt dephosphorylation in normal human dermal fibroblasts, and it attenuated skin fibrosis in mice models of systemic sclerosis

Kozo Nakai[a,*], Sakiko Karita[b], Junske Igarashi[c], Ikuko Tsukamoto[d], Katsuya Hirano[e], Yasuo Kubota[a]

[a] Department of Dermatology, Kagawa University, Kagawa, Japan
[b] School of Medicine, Kagawa University, Kagawa, Japan
[c] Department of Clinical Engineering, Morinomiya University of Medical Sciences, Osaka, Japan
[d] Department of Pharmaco-Bio-Informatics, Kagawa University, Kagawa, Japan
[e] Department of Cardiovascular Physiology, Kagawa University, Kagawa, Japan

ARTICLE INFO

Article history:
Received 10 December 2018
Received in revised form 19 February 2019
Accepted 21 February 2019

Keywords:
COA-Cl
TGF-β1
CTGF
Akt
Angiotensin II

ABSTRACT

Background: Systemic sclerosis (SSc) is characterized by fibrosis of the skin and internal organs. Although transforming growth factor (TGF)-β1-induced connective tissue growth factor (CTGF/CCN2) expression has been presented in SSc fibrosis, the therapeutic potential of targeting CTGF in SSc has not been fully explored. COA-Cl is a novel nucleic acid analog, which is reported to have pleiotropic beneficial biologic effects.

Objective: We examine the effects of COA-Cl on TGF-β1-induced CTGF expression in normal human dermal fibroblast (NHDF). We also examined the effects of COA-Cl on CTGF expression in a mouse SSc model of angiotensin II (Ang II)-induced skin fibrosis.

Methods: NHDF was cultured for *in vitro* experiments. For *in vivo* experiments, C57BL/6J mice were treated with Ang II for 14 days by subcutaneous osmotic pump. Quantitative real-time polymerase chain reaction, western blot analysis, immunohistochemical staining and immunofluorescence staining were performed to examine the expression levels of CTGF and phosphorylation levels of Smad2/3, ERK1/2 and Akt.

Results: COA-Cl attenuated the TGF-β1-induced expression of both CTGF mRNA and protein in NHDF. Although COA-Cl did not alter the TGF-β1-induced phosphorylation of Smad2/3 or ERK1/2, it reduced the TGF-β1-induced phosphorylation levels of Akt in NHDF. Notably, COA-Cl dephosphorylated the Akt of lysates of TGF-β1-treated NHDF. COA-Cl reduced the levels of CTGF mRNA, CTGF protein, dermal thickness, collagen content and Akt phosphorylation in the skin of mice SSc model.

Conclusion: These results imply that the inhibition of TGF-β1-induced CTGF expression by COA-Cl may be a therapeutic approach for SSc.

1. Introduction

Systemic sclerosis (SSc) is a multisystem connective tissue disorder that causes fibrosis of the skin and internal organs [1]. Connective tissue growth factor (CTGF, also known as CCN2), a member of the CCN family of matricellular proteins, is well-known as a key regulator of fibrosis in multiple tissues, including skin, heart, lung, liver, and kidney [2]. Both transforming growth factor (TGF)-β and CTGF are necessary for the sustained fibrosis [3]. Accumulating reports show that CTGF is highly expressed in SSc [4], and elevated CTGF protein expression has been observed in skin fibroblasts of the patient with SSc [5].

COA-Cl (6-amino-2-chloro-9-[trans-trans-2,3- bis(hydroxymethyl)cyclobutyl]purine) is a recently synthesized novel nucleic acid analog, which has adenosine-like structure [6]. There are some reports showing beneficial effects of COA-Cl in *in vitro* and *in vivo* experiments. COA-Cl exerts neuroprotective effects in both *in vitro* and *in vivo* ischemia models, which is mediated by ERK1/2 and purinergic receptors, and specifically P2X receptors *in vitro* [7]. Local administration of COA-Cl in rats reduced perihematomal edema in intracerebral hemorrhage and attenuated neurological

* Corresponding author at: Department of Dermatology, Faculty of Medicine, Kagawa University, 1750-1 Ikenobe, Miki-cho, Kita-gun, Kagawa, 761-0793, Japan.
E-mail address: kozo@kms.ac.jp (K. Nakai).

https://doi.org/10.1016/j.jdermsci.2019.02.003
0923-1811/

motor deficits by ameliorating oxidative stress [8]. In addition to its neuroprotective effects, COA-Cl also induces angiogenesis and synaptogenesis *via* ERK activation in both *in vivo* and *in vitro* models [7,9]. COA-Cl increases vascular endothelial growth factor (VGEF) expression in normal human dermal fibroblast (NHDF) [10]. More recently, it has been reported that COA-Cl has an inhibitory effect on TGF-β1-induced epithelial–mesenchymal transition (EMT) in RLE/Abca3 cells *via* suppression of ZEB2 mRNA expression [11].

These reports let us investigate the effects of COA-Cl on TGF-β1-induced CTGF expression in NHDF and the efficacy of COA-Cl as a potential therapeutic agent for SSc using a murine model of angiotensin II (Ang II)-induced skin fibrosis.

2. Materials and methods

2.1. Cell culture and drug treatment

NHDF were obtained from Kurabo (Osaka, Japan). They were maintained in culture using Dulbecco's modified Eagle's medium with 10% heat-inactivated fetal calf serum in a humidified incubator at 37 °C, perfused with 5% CO_2. TGF-β1 was purchased from Cell Signaling Technology (Danvers, MA, USA). LY294002 was purchased from Calbiochem-Novabiochem (San Diego, CA, USA). COA-Cl was synthesized as previously described [9]. COA-Cl is now commercially available as 2-Cl-C.OXT-A from FUJIFILM WAKO Pure Chemical Corporation (Osaka, Osaka, Japan). After 24h' treatment with TGF-β1, cells were harvested for Western blot analysis or RT-PCR analysis. For *in vitro* experiments, COA-Cl or LY294002 was added 30 min before treatment with TGF-β1. For *ex vitro* experiments, COA-Cl was added to the harvested cell protein mixture, and the protein mixture was incubated for 1 h at 37 °C.

2.2. Mice and treatments

All animal experiments and methods were approved by the Kagawa University Institutional Animal Care and Use Committee. C57BL/6J male mice were handled in compliance with the guidelines for conducting Animal Experiments at Kagawa University. The mice were housed in a SPF facility at the Health Science Center of Kagawa University under controlled temperature (23 °C) and humidity (55%). The mice were given food and water *ad libitum* (MF: Oriental Yeast Co., Itabashi, Tokyo, Japan). Alzet osmotic miniature pumps (Model 1002, DURECT, Cupertino, CA, USA) delivering Ang II (Sigma-Aldrich, St. Louis, MO, USA) at a rate of 1000 ng/kg/minutes (pressure dose) with/without COA-Cl at a rate of 8000 ng/kg/minutes or PBS, were implanted subcutaneously on the back of 4-week-old mice, as described previously [12]. After 2 weeks, the mice were sacrificed by intraperitoneal sodium pentobarbital (1 g/kg) injection, and the skin surrounding the pump outlet was collected.

2.3. Western blot analysis

Cells were washed with PBS. Then, RIPA buffer containing 1% v/v NP40, 20 mM Tris (pH 7.7), 150 mM NaCl, 1 mM EDTA and a mixture of protease inhibitors (Calbiochem, San Diego, CA, USA) was added. Skin tissue specimens were homogenized with a Polytron homogenizer in RIPA buffer and a mixture of protease inhibitors. After incubation at 4 °C for 20 min, the samples were sonicated on ice and centrifuged at 14,000 rpm for 10 min. The protein concentration of the supernatants was analyzed using the BCA protein assay (Pierce, Rockford, IL, USA). An equal amount of protein was separated on SDS-PAGE gel and transferred to a PVDF membrane. The membrane was then probed with primary antibodies. The anti-CTGF antibody was purchased from Gene Tex (Irvine, CA, USA). Antibodies against phospho-Smad2/3 and Smad2/3 were purchased from R&D systems (Minneapolis, MN, USA). Antibodies against phospho-Akt, Akt, phospho-ERK1/2, ERK1/2, GAPDH and β-actin were purchased from Cell Signaling Technology (Danvers, MA, USA). Membrane-bound primary antibodies were visualized using the appropriate secondary antibodies conjugated to horseradish peroxidase and a chemiluminescent substrate (Pierce, Rockford, IL, USA). The immunoreactive signals from the chemiluminescent substrate were visualized by exposure to standard X-ray films. Images were subjected to densitometric analysis using the Image J software (National Institutes of Health, Bethesda, MD, USA).

2.4. Quantitative RT-PCR

Total RNA was extracted from the skin tissues using Rneasy mini column (Qiagen, Vlencia, CA, USA) or TRIzol reagent (Invitrogen, Carlsbad, CA, USA). Conventional RT-PCR assay were performed as described [13]. Primers for RT-PCR analysis were follows: human CTGF sense 5′−CCTGCAGGCTAGAGAAGCAG-3′, human CTGF anti-sense 5′-TGGAGATTTTGGGAGTACGG-3′, human GAPDH sense 5′-ACCACAGTCCATGCCATCAC-3′and human GAPDH anti-sense 5′-TCCACCACCCTGTTGCTGTA-3′. The resulting PCR product was separated on a 2% agarose gel and visualized with ethidium bromide under ultraviolet light. Gel images were captured with a CCD camera system and subjected to densitometric analyses using NIH image software 1.63. We optimized the assay conditions and verified that increasing amounts of a starting mRNA sample yield increasing amounts of RT-PCR product under these conditions in each primer pair.

Quantitative RT-PCR was performed using the Taqman gene expression assay system (Applied Biosystems, Foster City, CA, USA). The following probes were used: Hs00170014_m1 (human CTGF), Mn01192933_g1, Hs99999903_m1 (human β-actin), and Mm00607939_s1 (mouse β-actin). Probes for β-actin were used as an endogenous control. Quantitative RT-PCR was carried out using StepOnePlus (Applied Biosystems, Foster City, CA, USA). Gene expression values were calculated based on the comparative threshold cycle method, normalized to β-actin expression, and displayed as a fold induction relative to the control.

2.5. Fluorescence detection of reactive oxygen species (ROS) by 2′,7′-dichlorofluorescein (DCF) staining

The ROS formation was assessed by DCF staining following supplier's protocol (Thermo Fisher Scientific, Waltham, MA, USA). After treating NHDF with TGFβ1, the medium was removed, and cells were washed with PBS. A final concentration of 25 μM DCF was added and incubated for 20 min. Cells were washed twice with PBS and maintained in a fresh PBS. Then fluorescence was detected using a fluorescence microplate reader, Fluoroskan Ascent FL® (Thermo Fisher Scientific, Waltham, MA, USA), at excitation and emission wavelengths of 444 and 538 nm. For the observation of cell images, a fluorescence microscope was operated at excitation and emission wavelengths of 450 and 520 nm, respectively.

2.6. Immunohistochemical analysis

Skin samples (1–2 cm^2) that were removed from the mid-dorsum of mice were directly fixed in 10% buffered formalin. Tissues were dehydrated and embedded in paraffin prior to cutting 2-5-μm thick sections. The samples were subsequently deparaffinized in xylene, rehydrated and immunostained with antibody against CTGF (1:200 dilution) using the Histofine simple stain reagent (Nichirei, Tokyo, Japan) according to the manufacturer's protocol. Briefly, endogenous peroxidase activity was blocked by

incubating the sections with 3% hydrogen peroxide for 5 min. After a wash with PBS, the sections were incubated with the primary antibodies at room temperature for 1 h, washed in PBS and subsequently incubated with peroxidase-conjugated secondary antibodies. After wash, sections were incubated in a 3-3′-diaminobenzidine tetrahydrochloride solution and counterstained with Mayer's hematoxylin.

2.7. Immunofluorescence microscopy on frozen tissue sections

Frozen tissue sections (30 μm) were cut and placed onto Superfrost plus slides. Sections were pre-blocked in a solution containing 1% BSA, 0.1% Triton X-100, and 1% gelatin in PBS. Antibody against phspho-Akt (1:200 dilution) were then added to a fresh solution and incubated with the samples at room temperature for 1 h. After washing the slides 3 times with PBS for 10 min each, the sections were incubated with fresh solution containing secondary Alexa Fluor 555-conjugated antibodies (1:400 dilution) for 30 min before washing and mounting. Nuclei were stained with TO-PRO-3. Sections were examined using a confocal microscope (LSM 700; Carl Zeiss, Jena, Thüringen, Germany).

2.8. Statistical analysis

Data are expressed as the mean ± S.E. Statistical analysis was performed by an analysis of variance followed by Mann-Whitney's *U* test P-values of < 0.05 were considered significant.

3. Results

3.1. COA-Cl attenuated the TGF-β1-induced CTGF expression in NHDF

RT-PCR analysis reveals that TGF-β1 (5 ng/ml) increased the expression levels of CTGF mRNA after 24 h in NHDF (Fig. 1A, B). Treatment with COA-Cl (100 μM) 30 min prior to TGF-β1 suppressed the increased levels of CTGF mRNA expression. Similarly, real time RT-PCR analysis also demonstrated that COA-Cl suppressed the TGF-β1-induced CTGF mRNA expression in NHDF (Fig. 1C). Western blot analysis revealed that COA-Cl suppressed the TGF-β1-induced CTGF protein expression in NHDF (Fig. 1D, E). These results suggest that COA-Cl suppressed the TGF-β1-induced CTGF expression at the level of transcription. Although TGF-β1 increased the expression levels of α-smooth muscle actin (α-SMA),

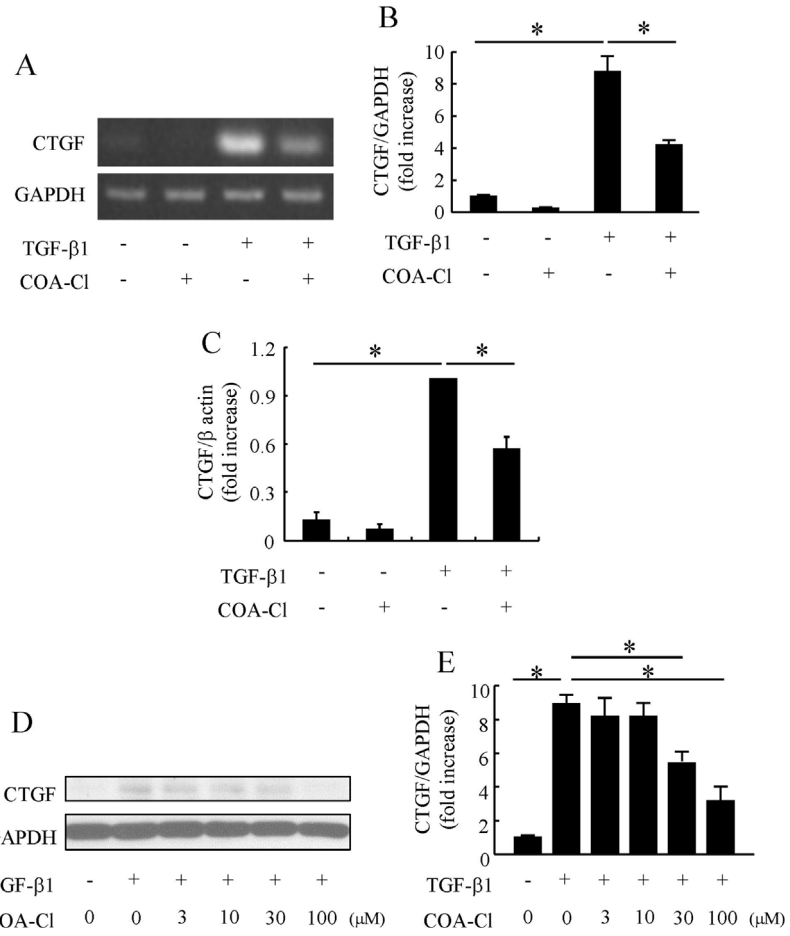

Fig. 1. COA-Cl attenuated the TGF-β1-induced CTGF expression in NHDF. (A–C) NHDF was treated with TGF-β1 (5 ng/ml) for 24 h. COA-Cl (100 μM) was added 30 min prior to TGF-β1 treatment. (A) Representative RT-PCR results of CTGF and GAPDH are shown. (B) Densitometric analysis results were obtained from pooled data. Relative mRNA expression normalized to GAPDH, arbitrary units (n = 5). (C) Real time RT-PCR analysis results of CTGF were obtained from pooled data. Relative mRNA expression normalized to β actin, arbitrary units (n = 4). (D, E) NHDF was treated with TGF-β1 (5 ng/ml) for 24 h. COA-Cl was added 30 min prior to TGF-β1 treatment at indicated concentrations. (D) Representative western blot results of CTGF and GAPDH are shown. (E) Densitometric analysis results were obtained from pooled data. Relative protein expression was normalized to GAPDH, arbitrary units (n = 4). Values represent the mean ± S.E. $^{*}P < 0.05$.

a marker of EMT, COA-Cl did not suppress the TGF-β1-induced α-SMA protein expression in NHDF (Suppl. Fig. 1).

3.2. COA-Cl attenuated the TGF-β1-induced Akt phosphorylation in NHDF

To elucidate the mechanism of the inhibition of TGF-β1-induced CTGF transcription by COA-Cl in NHDF, we first examined Smad2/3 phosphorylation, because Smad2/3 signaling pathways are popular in TGF-β1-regulated various gene expressions [14]. Although TGF-β1 increased the levels Smad2/3 phosphorylation, COA-Cl did not prevent the increase in the levels of these phosphorylations (Fig. 2A, B). Cross-talk between ERK1/2 and Smad signaling pathways following stimulation from TGF-β occurs in several cells [15–17]. TGF-β1 up-regulates CTGF expression in human granulosa cells through Smad and ERK1/2 signaling pathways [18]. However, in our experimental conditions, TGF-β1 did not enhance the phospholylation levels of ERK1/2, and COA-Cl did not alter the phosphorylation levels of ERK1/2 in NHDF (Fig. 2C, D). We next focused on Smad-independent signaling pathways to explore other possible signaling pathways that are involved in the inhibition of TGF-β1-induced CTGF expression in NHDF. It has been reported that PI3K signaling pathway is involved in the TGF-β1-induced CTGF expression in human lung epithelial cells [19]. Therefore, we examined the phospholylation levels of Akt in NHDF. As shown in Fig. 2E, F, TGF-β1 enhanced the phospholylation levels of Akt, and COA-Cl decreased the phosphorylation levels in NHDF. We also confirmed that LY294002, a PI3K/Akt inhibitor, inhibited TGF-β1-induced CTGF protein expression in NHDF (Fig. 2G, H). These results suggest that COA-Cl inhibited the TGF-β1-induced activation of PI3K signaling pathway in NHDF.

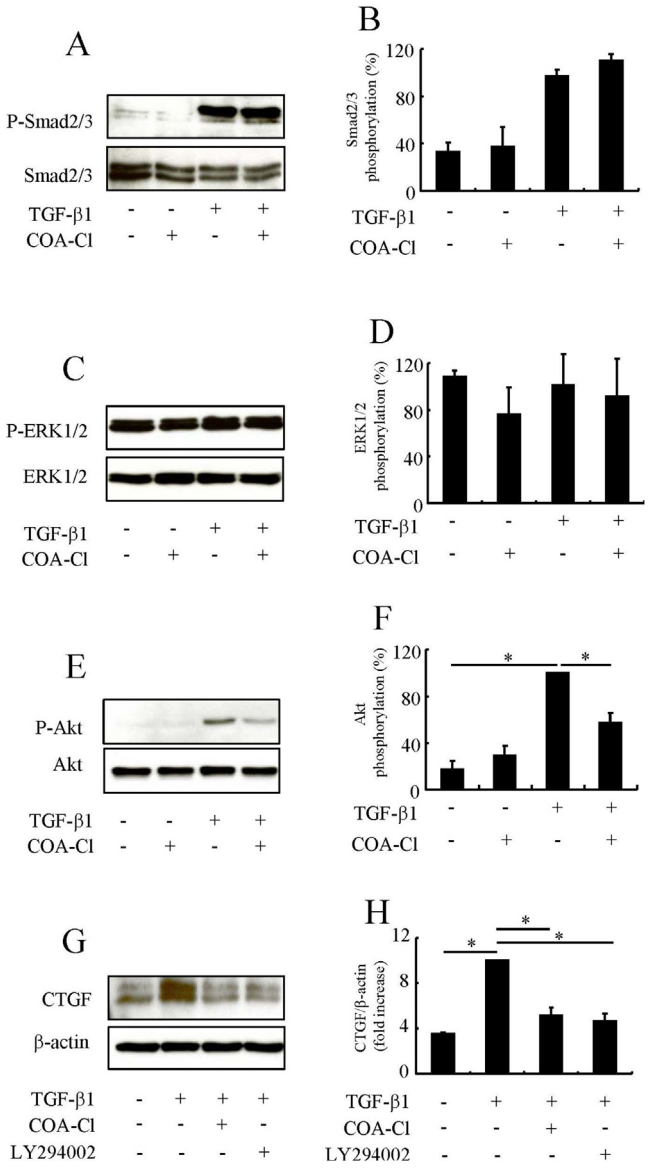

Fig. 2. COA-Cl attenuated the TGF-β1-induced Akt phosphorylation in NHDF. NHDF was treated with TGF-β1 (5 ng/ml) for 24 h. COA-Cl (100 μM) or LY294002 (10 μM) was added 30 min prior to TGF-β1 treatment. (A, C, E, G) Representative western blot results of phospho Smad2/3, Smad2/3, phospho ERK1/2, ERK1/2, phospho Akt, Akt, CTGF and β-actin are shown. (B, D, F, H) Densitometric analysis results were obtained from pooled data. Relative protein phosphorylation levels were normalized to each total protein, arbitrary units. Values represent the mean ± S. E. (n = 4). *$P < 0.05$.

3.3. COA-Cl dephosphorylated Akt of TGF-β1-treated NHDF cell lysates

To clarify that COA-Cl directly attenuated the TGF-β1-induced Akt phosphorylation in NHDF, we added COA-Cl to TGF-β1-treated NHDF cell lysates. The phospholyration levels of Smad2/3 and ERK1/2 were not altered by the addition of COA-Cl to the cell lysates of TGF-β1-treated NHDF (Fig. 3A–D). However, COA-Cl dephospholyrated Akt of the cell lysates of TGF-β1-treated NHDF (Fig. 3E, F). These results were consistent with *in vitro* experiments, and suggest that COA-Cl directly attenuated the TGF-β1-induced Akt phosphorylation in NHDF.

3.4. COA-Cl attenuated the TGF-β1-induced ROS formation in NHDF

TGF-β1 is known to increase ROS formation *via* several pathways including PI3K signaling pathway [20–22]. Thus, we examined the effects of COA-Cl on the TGF-β1-induced ROS formation in NHDF. As shown in Fig. 4A, TGF-β1 increased the ROS formation in NHDF, and COA-Cl decreased the TGF-β1-induced ROS formation dose dependently. By using a fluorescence microscope, we detected high signal levels of ROS in TGF-β1-treated NHDF, and the signal levels were reduced by the addition of COA-Cl (Fig. 4B).

3.5. COA-Cl attenuated the CTGF expression with Akt phosphorylation, and improved skin fibrosis in the skin of a mouse model of SSc

To evaluate the therapeutic effects of COA-Cl in the *in vivo* model of SSc, we used a mouse model of Ang II-induced skin fibrosis [12]. Ang II has been shown to activate the TGF-β signaling pathway and increase the CTGF expression levels in the skin. The useful therapeutic effects of CTGF blockade by using a monoclonal antibody has been demonstrated in the mouse model of Ang II-induced skin fibrosis [23]. Similarly, we found that the increased levels of Ang II-induced CTGF mRNA expression were attenuated by treating with COA-Cl (Fig. 5A). COA-Cl reduced dermal thickness and collagen content in the skin of Ang II-treated mice (Fig. 5B, C). COA-Cl also reduced the CTGF protein expression and phosphorylation of Akt in the dermis of Ang II-treated mice (Fig. 5D, E). Although the expression levels of α-SMA were increased in the skin of Ang II-treated mice, COA-Cl did not suppress the Ang II-induced α-SMA protein expression (Suppl. Fig. 2).

4. Discussion

Only limited treatment options are now available for patients with SSc. COA-Cl is a novel nucleic acid analog. Beneficial effects of COA-Cl have been reported in various types of cells and some animal models of diseases [7–11]. In the current study, we

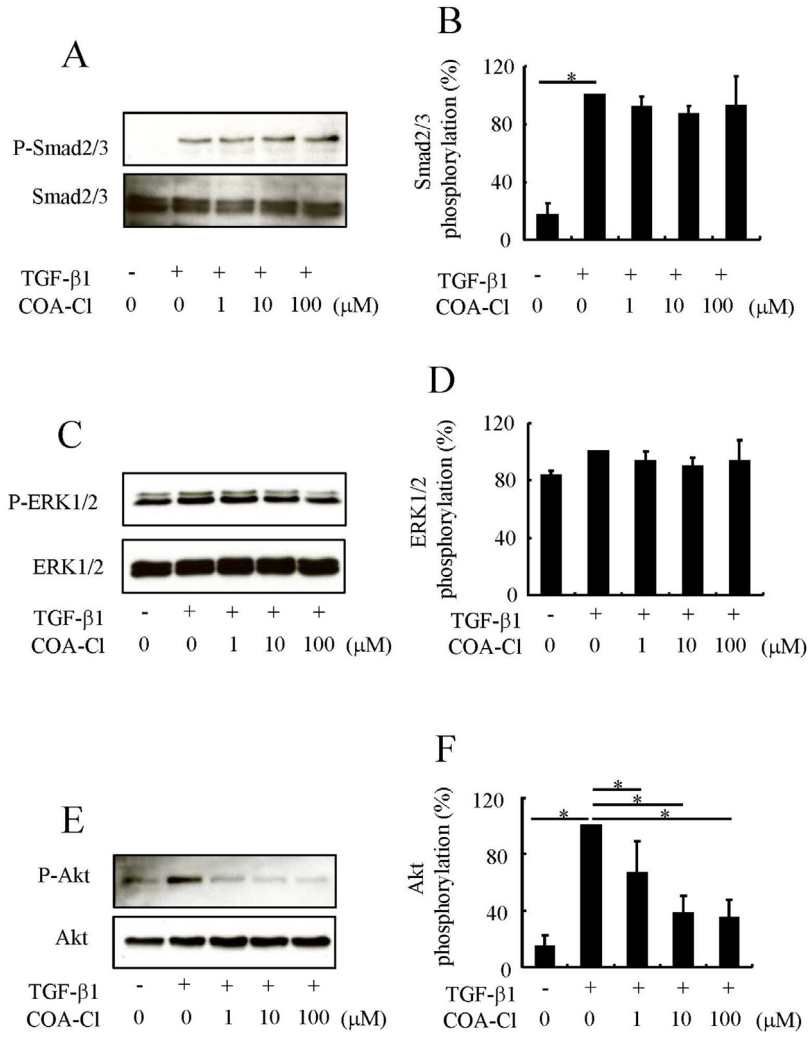

Fig. 3. COA-Cl dephosphorylated Akt of TGF-β1-treated NHDF cell lysates. COA-Cl was added to TGF-β1-treated NHDF cell lysates as indicated concentrations. (A, C, E) Representative western blot results of phospho Smad2/3, Smad2/3, phospho ERK1/2, ERK1/2, phospho Akt and Akt are shown. (B, D, F) Densitometric analysis results were obtained from pooled data. Relative protein phosphorylation levels were normalized to each total protein, arbitrary units. Values represent the mean ± S.E. (n = 4). $^{*}P < 0.05$.

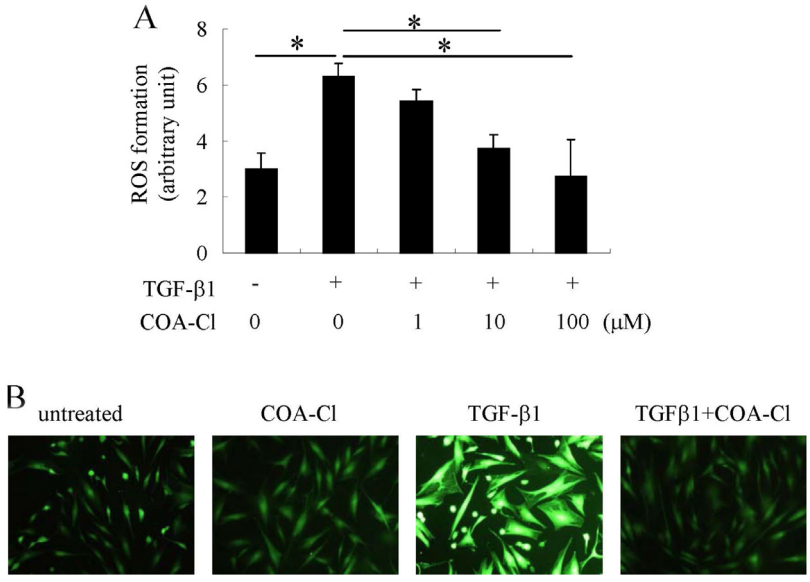

Fig. 4. COA-Cl attenuated the TGF-β1-induced ROS formation in NHDF. The ROS formation was assessed by DCF staining. (A) Summary of fluorescence data obtained by using a fluorescence microplate reader. Values represent the mean ± S.E. (n = 6). $^{*}P < 0.05$.
(B) Representative fluorescence microscopic images at ×400 were shown.

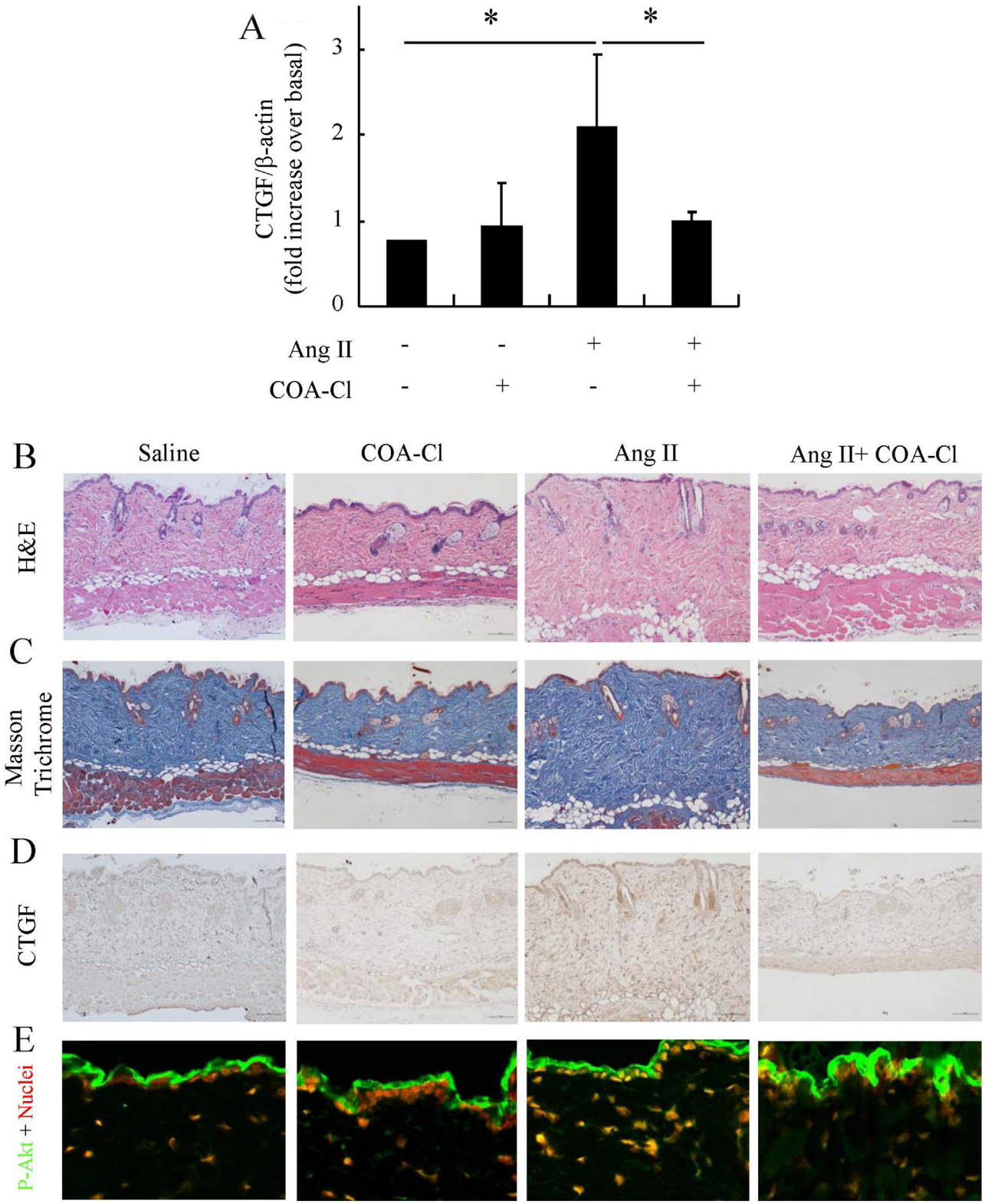

Fig. 5. COA-Cl attenuated the CTGF expression with Akt dephosphorylation, and improved skin fibrosis in the skin of a mouse model of SSc. Osmotic miniature pumps delivering Ang II at a rate of 1000 ng/kg/minutes with/without COA-Cl at a rate of 8000 ng/kg/minutes or PBS were implanted subcutaneously on the back of 4-week-old mice. After 2 weeks, the skin surrounding the pump outlet was collected. (A) Real time RT-PCR analysis results of CTGF were obtained from pooled data. Relative mRNA expression normalized to β actin, arbitrary units (n = 4). (B) H & E staining at ×20. (C) Masson Trichrome staining at ×20. (D) Immunostaining for CTGF at ×20. (E) Immunofluorescent staining for phospho Akt (green) and nuclei stained with TO-PRO-3 (red) at ×40.

examined the effects of COA-Cl on CTGF expression in TGF-β1-treated NHDF and AngII-induced mouse model of SSc. COA-Cl attenuated the both TGF-β1-induced CTGF mRNA and protein expressions by inhibiting Akt activation in NHDF. COA-Cl reduced the dermal thickness, collagen content, CTGF expression and Akt phosphorylation levels in the skin of Ang II-treated mice. These results imply that the inhibition of TGF-β1-induced CTGF expression by COA-Cl can be a therapeutic approach for the treatment of SSc.

Expression of the profibrotic protein CTGF correlates well with the severity of fibrotic phenotype of SSc [24]. CTGF is not normally expressed in fibroblasts unless induced by some stimuli such as TGF-β. Smads have been believed to play a crucial role in mediating the intracellular responses to TGF-β and/or its related factors [25]. Smads work as transcription factors that constantly shuttle between the cytoplasm and the nucleus [26]. Among them, Smad2/3 signaling pathways play a major role in TGF-β1-regulated various gene expressions [14]. We have confirmed that TGF-β1 increased the levels of Smad2/3 phosphorylation. However, COA-Cl did not prevent the increase in the levels of these phosphorylation. TGF-β1 is known to activate canonical and non-canonical signaling pathways. The canonical pathway activates the downstream signaling molecules Smad2/3. The non-canonical signaling pathway, which is called the non-Smad signaling pathway, involves the activation of ERK, Akt and Rho GTPase signaling pathways [27]. In our study, treatment with TGF-β1 for 24 h did not elevate the phospholylation levels of ERK1/2, and COA-Cl did not alter the phosphorylation levels of ERK1/2 in NHDF. This may be explained by the kinetics of ERK phosphorylation induced by TGF-β1. It varies with cell types and culture conditions, but the activation of ERK appears to occur rapidly within 5–10 min of TGF-β1 stimulation in fibroblast [28]. Instead COA-Cl might activate ERK in fibroblast as well as primary cortical neuron [7]. Several reports suggest a role of PI3K in TGF-β signaling. TGF-β can activate PI3K, as indicated by the phosphorylation of its downstream effector Akt. This activation appears to be independent of Smad2/3 activation [29]. Clinically, the significance of Akt in SSc skin fibroblasts has been indicated, and Akt of fibroblasts from SSc patients have been highly activated [30]. Akt is known for its anti-apoptotic ability that interferes with both death receptor and mitochondrial pathways [31], and the anti-apotoic ability of SSc fibroblasts may contribute to the activation of fibroblasts in the skin promoting the extracellular matrix deposition. Recently, it has been reported that COA-Cl suppressed the TGF-β1 mediated ZEB2 mRNA expression and EMT in RLE/Abca3 cells [11]. ZEB2 is a transcriptional co-repressor for TGF-β signaling pathway through binding to Smad proteins. ZEB2 plays an important role in human and mice fibrosis [32]. The bleomycin-induced skin fibrosis was attenuated in mice with a mesoderm-specific deletion of the *Zeb2* gene. However, COA-Cl did not suppress the TGF-β1-induced Smad2/3 phosphorylations in NHDF. In addition, COA-Cl did not suppress the TGF-β1-induced α-SMA protein expression in NHDF, and COA-Cl did not suppress the Ang II-induced α-SMA protein expression in the skin of mice. These results suggest that COA-Cl could not inhibit TGF-β1-induced ZEB2 expression and EMT. Both Samd2/3 and Akt may be involved in TGF-β1-induced EMT. Presumably, the inhibition of Akt phosphorylation alone could not inhibit TGF-β1-induced EMT.

In the current study, we have demonstrated that COA-Cl dephospholyrated Akt of the cell lysates of TGF-β1-treated NHDF. The phospholyration levels of Smad2/3 and ERK1/2 were not altered by the addition of COA-Cl to the cell lysates of TGF-β1-treated NHDF. These results suggest that the possible effects of COA-Cl as a potent allosteric Akt inhibitor. However, the real chemistry still remains unclear at this stage. COA-Cl has been shown to reduce oxidative stress in acute phase of intracerebral hemorrhage [8]. We found that COA-Cl suppressed TGF-β1-induced ROS formation in NHDF. TGF-β1 is known to increase ROS formation *via* several pathways. Among them, Akt appears to be a key mediator of ROS formation [33,34]. Considering the allosteric Akt inhibiting effects of COA-Cl, COA-Cl suppressed the TGF-β1-induced ROS formation by inhibiting Akt in NHDF. Alternatively, it is possible that COA-Cl suppressed ROS formation by increasing the expression levels of peroxisome proliferator-activated receptor gamma co-activator (PGC)-1α in NHDF. TGF-β1 induces ROS formation, and decreases the expression of catalase (CAT) and superoxide dismutase (SOD), antioxidant enzymes [20,35]. PGC-1α has been reported to increase the expression of CAT and SOD [36,37]. Igarashi et al. reported that the expression levels of PGC-1α were increased by the treatment of COA-Cl in NHDF [10].

We have utilized a mouse model of SSc induced by Ang II [12,23]. As well as the bleomycin-induced models of skin fibrosis [38], Ang II induces dermal fibrosis through diverse pathogenic mechanisms, including stimulation of collagen and CTGF synthesis, myofibroblast differentiation, and recruitment of fibrocytes [12]. Increased number of infiltrating fibrocytes is considered to contribute to the development of dermal fibrosis in the skin of Ang II-infused mice [12]. The interaction between Ang II and TGF-β in the induction of fibrosis is well characterized in many organs such as kidney and heart [39,40]. Thus, COA-Cl might prevent the TGF-β1-mediated dermal fibrosis in the skin of Ang II-treated mice. Moreover, recent studies suggest the important roles of CTGF in the development of skin fibrosis [41]. Blocking CTGF by human anti-CTGF antibody, FG-3019, prevented the development of skin fibrosis in response to Ang II challenge in mouse [23]. Therapeutic effects of FG-3019 were also reported in bleomycin-induced lung fibrosis of mouse [42]. Similarly, we have demonstrated that COA-Cl inhibited CTGF mRNA expression in the skin and prevented the development of skin fibrosis in response to Ang II challenge in mouse.

In summary, we have demonstrated the inhibitory effects of COA-Cl on TGF-β1-induced CTGF expression and Ang II-induced dermal fibrosis in mouse. These results suggest the therapeutic effects of COA-Cl on the fibrotic process of SSc.

Funding

None.

Conflict of interest

The authors have no conflict of interest to declare.

Acknowledgments

This study was supported by the Grants-in-Aid for scientific research for K. Y (17K10210) from the Ministry of Education, Science, Sports, and Culture, Japan.

Appendix A. Supplementary data

Supplementary material related to this article can be found, in the online version, at doi:https://doi.org/10.1016/j.jdermsci.2019.02.003.

References

[1] Y. Allanore, R. Simms, O. Distler, M. Trojanowska, J. Pope, C.P. Denton, J. Varga, Systemic sclerosis, Nat. Rev. Dis. Primers 1 (2015) 15002.
[2] A. Leask, S.K. Parapuram, X. Shi-Wen, D.J. Abraham, Connective tissue growth factor (CTGF, CCN2) gene regulation: a potent clinical bio-marker of fibroproliferative disease? J. Cell Commun. Signal. 3 (2009) 89–94.

[3] T. Mori, S. Kawara, M. Shinozaki, N. Hayashi, T. Kakinuma, A. Igarashi, M. Takigawa, T. Nakanishi, K. Takehara, Role and interaction of connective tissue growth factor with transforming growth factor-beta in persistent fibrosis: a mouse fibrosis model, J. Cell. Physiol. 181 (1999) 153–159.
[4] L.M. Rice, J. Ziemek, E.A. Stratton, S.R. McLaughlin, C.M. Padilla, A.L. Mathes, R. B. Christmann, G. Stifano, J.L. Browning, M.L. Whitfield, R.F. Spiera, J.K. Gordon, R.W. Simms, Y. Zhang, R. Lafyatis, A longitudinal biomarker for the extent of skin disease in patients with diffuse cutaneous systemic sclerosis, Arthritis. Rheumatol. 67 (2015) 3004–3015.
[5] A. Holmes, D.J. Abraham, Y. Chen, C. Denton, X. Shi-wen, C.M. Black, A. Leask, Constitutive connective tissue growth factor expression in scleroderma fibroblasts is dependent on Sp1, J. Biol. Chem. 278 (2003) 41728–41733.
[6] N. Sakakibara, J. Igarashi, M. Takata, Y. Demizu, T. Misawa, M. Kurihara, R. Konishi, Y. Kato, T. Maruyama, I. Tsukamoto, Synthesis and evaluation of novel carbocyclic oxetanocin a (COA-Cl) derivatives as potential tube formation agents, Chem. Pharm. Bull. (Tokyo) 63 (2015) 701–709.
[7] N. Okabe, E. Nakamura, N. Himi, K. Narita, I. Tsukamoto, T. Maruyama, N. Sakakibara, T. Nakamura, T. Itano, O. Miyamoto, Delayed administration of the nucleic acid analog 2Cl-C.OXT-A attenuates brain damage and enhances functional recovery after ischemic stroke, Brain Res. 1506 (2013) 115–131.
[8] F. Lu, T. Nakamura, N. Okabe, N. Himi, E. Nakamura-Maruyama, T. Shiromoto, K. Narita, I. Tsukamoto, G. Xi, R.F. Keep, O. Miyamoto, COA-Cl, a novel synthesized nucleoside analog, exerts neuroprotective effects in the acute phase of intracerebral hemorrhage, J. Stroke Cerebrovasc. Dis. 25 (2016) 2637–2643.
[9] I. Tsukamoto, N. Sakakibara, T. Maruyama, J. Igarashi, H. Kosaka, Y. Kubota, M. Tokuda, H. Ashino, K. Hattori, S. Tanaka, M. Kawata, R. Konishi, A novel nucleic acid analogue shows strong angiogenic activity, Biochem. Biophys. Res. Commun. 399 (2010) 699–704.
[10] J. Igarashi, R. Okamoto, T. Yamashita, T. Hashimoto, S. Karita, K. Nakai, Y. Kubota, M. Takata, F. Yamaguchi, M. Tokuda, N. Sakakibara, I. Tsukamoto, R. Konishi, K. Hirano, A key role of PGC-1alpha transcriptional coactivator in production of VEGF by a novel angiogenic agent COA-Cl in cultured human fibroblasts, Physiol. Rep. 4 (2016).
[11] M. Kawami, J. Deguchi, R. Yumoto, N. Sakakibara, I. Tsukamoto, R. Konishi, M. Takano, Effect of COA-Cl on transforming growth factor-beta1-induced epithelial-mesenchymal transition in RLE/Abca3 cells, Drug Metab. Pharmacokinet. 32 (2017) 224–227.
[12] L. Stawski, R. Han, A.M. Bujor, M. Trojanowska, Angiotensin II induces skin fibrosis: a novel mouse model of dermal fibrosis, Arthritis Res. Ther. 14 (2012) R194.
[13] K. Nakai, Y. Kubota, H. Kosaka, Inhibition of nuclear factor kappa B activation and inducible nitric oxide synthase transcription by prolonged exposure to high glucose in the human keratinocyte cell line HaCaT, Br. J. Dermatol. 150 (2004) 640–646.
[14] K.A. Brown, J.A. Pietenpol, H.L. Moses, A tale of two proteins: differential roles and regulation of Smad2 and Smad3 in TGF-beta signaling, J. Cell. Biochem. 101 (2007) 9–33.
[15] T. Hayashida, M. Decaestecker, H.W. Schnaper, Cross-talk between ERK MAP kinase and Smad signaling pathways enhances TGF-beta-dependent responses in human mesangial cells, FASEB J. 17 (2003) 1576–1578.
[16] Y. Zhu, H. Tao, C. Jin, Y. Liu, X. Lu, X. Hu, X. Wang, Transforming growth factor-beta1 induces type II collagen and aggrecan expression via activation of extracellular signal-regulated kinase 1/2 and Smad2/3 signaling pathways, Mol. Med. Rep. 12 (2015) 5573–5579.
[17] X. Wang, Y. Zhu, H. Tao, C. Jin, Y. Liu, X. Lu, X. Hu, C. Fan, Interaction of ERK1/2 and Smad2/3 signaling pathways in TGF-beta1-induced TIMP-3 expression in rat chondrocytes, Arch. Biochem. Biophys. 564 (2014) 229–236.
[18] J.C. Cheng, H.M. Chang, L. Fang, Y.P. Sun, P.C. Leung, TGF-beta1 up-regulates connective tissue growth factor expression in human granulosa cells through Smad and ERK1/2 signaling pathways, PLoS One 10 (2015)e0126532.
[19] L. Shi, N. Dong, X. Fang, X. Wang, Regulatory mechanisms of TGF-beta1-induced fibrogenesis of human alveolar epithelial cells, J. Cell. Mol. Med. 20 (2016) 2183–2193.
[20] R.M. Liu, L.P. Desai, Reciprocal regulation of TGF-beta and reactive oxygen species: a perverse cycle for fibrosis, Redox Biol. 6 (2015) 565–577.
[21] S. Ismail, A. Sturrock, P. Wu, B. Cahill, K. Norman, T. Huecksteadt, K. Sanders, T. Kennedy, J. Hoidal, NOX4 mediates hypoxia-induced proliferation of human pulmonary artery smooth muscle cells: the role of autocrine production of transforming growth factor-{beta}1 and insulin-like growth factor binding protein-3, Am. J. Physiol. Lung Cell Mol. Physiol. 296 (2009) L489–99.
[22] C. Michaeloudes, M.B. Sukkar, N.M. Khorasani, P.K. Bhavsar, K.F. Chung, TGF-beta regulates Nox4, MnSOD and catalase expression, and IL-6 release in airway smooth muscle cells, Am. J. Physiol. Lung Cell Mol. Physiol. 300 (2011) L295–304.
[23] K. Makino, T. Makino, L. Stawski, K.E. Lipson, A. Leask, M. Trojanowska, Anti-connective tissue growth factor (CTGF/CCN2) monoclonal antibody attenuates skin fibrosis in mice models of systemic sclerosis, Arthritis Res. Ther. 19 (2017) 134.
[24] A. Igarashi, K. Nashiro, K. Kikuchi, S. Sato, H. Ihn, G.R. Grotendorst, K. Takehara, Significant correlation between connective tissue growth factor gene expression and skin sclerosis in tissue sections from patients with systemic sclerosis, J. Invest. Dermatol. 105 (1995) 280–284.
[25] R. Derynck, Y. Zhang, Intracellular signalling: the mad way to do it, Curr. Biol. 6 (1996) 1226–1229.
[26] B. Schmierer, C.S. Hill, TGFbeta-SMAD signal transduction: molecular specificity and functional flexibility, Nat. Rev. Mol. Cell Biol. 8 (2007) 970–982.
[27] Y.E. Zhang, Non-Smad pathways in TGF-beta signaling, Cell Res. 19 (2009) 128–139.
[28] I. Mucsi, K.L. Skorecki, H.J. Goldberg, Extracellular signal-regulated kinase and the small GTP-binding protein, Rac, contribute to the effects of transforming growth factor-beta1 on gene expression, J. Biol. Chem. 271 (1996) 16567–16572.
[29] M.C. Wilkes, H. Mitchell, S.G. Penheiter, J.J. Dore, K. Suzuki, M. Edens, D.K. Sharma, R.E. Pagano, E.B. Leof, Transforming growth factor-beta activation of phosphatidylinositol 3-kinase is independent of Smad2 and Smad3 and regulates fibroblast responses via p21-activated kinase-2, Cancer Res. 65 (2005) 10431–10440.
[30] J.B. Jun, M. Kuechle, J. Min, S.C. Shim, G. Kim, V. Montenegro, J.H. Korn, K.B. Elkon, Scleroderma fibroblasts demonstrate enhanced activation of Akt (protein kinase B) in situ, J. Invest. Dermatol. 124 (2005) 298–303.
[31] S.R. Datta, A. Brunet, M.E. Greenberg, Cellular survival: a play in three Akts, Genes Dev. 13 (1999) 2905–2927.
[32] M. Teraishi, M. Takaishi, K. Nakajima, M. Ikeda, Y. Higashi, S. Shimoda, Y. Asada, A. Hijikata, O. Ohara, Y. Hiraki, S. Mizuno, T. Fukada, T. Furukawa, N. Wakamatsu, S. Sano, Critical involvement of ZEB2 in collagen fibrillogenesis: the molecular similarity between Mowat-Wilson syndrome and Ehlers-Danlos syndrome, Sci. Rep. 7 (2017) 46565.
[33] I. Dolado, A.R. Nebreda, AKT and oxidative stress team up to kill cancer cells, Cancer Cell 14 (2008) 427–429.
[34] V. Nogueira, Y. Park, C.C. Chen, P.Z. Xu, M.L. Chen, I. Tonic, T. Unterman, N. Hay, Akt determines replicative senescence and oxidative or oncogenic premature senescence and sensitizes cells to oxidative apoptosis, Cancer Cell 14 (2008) 458–470.
[35] E.J. Sohn, J. Kim, Y. Hwang, S. Im, Y. Moon, D.M. Kang, TGF-beta suppresses the expression of genes related to mitochondrial function in lung A549 cells, Cell. Mol. Biol. (Noisy-le-grand) (Suppl. 58) (2012) OL1763-7.
[36] S. Baldelli, K. Aquilano, M.R. Ciriolo, PGC-1alpha buffers ROS-mediated removal of mitochondria during myogenesis, Cell Death Dis. 5 (2014)e1515.
[37] J. Iacovelli, G.C. Rowe, A. Khadka, D. Diaz-Aguilar, C. Spencer, Z. Arany, M. Saint-Geniez, PGC-1alpha induces human RPE oxidative metabolism and antioxidant capacity, Invest. Ophthalmol. Vis. Sci. 57 (2016) 1038–1051.
[38] S. Liu, R. Taghavi, A. Leask, Connective tissue growth factor is induced in bleomycin-induced skin scleroderma, J. Cell Commun. Signal. 4 (2010) 25–30.
[39] S.A. Mezzano, M. Ruiz-Ortega, J. Egido, Angiotensin II and renal fibrosis, Hypertension 38 (2001) 635–638.
[40] S. Rosenkranz, TGF-beta1 and angiotensin networking in cardiac remodeling, Cardiovasc. Res. 63 (2004) 423–432.
[41] S. Kubota, M. Takigawa, Cellular and molecular actions of CCN2/CTGF and its role under physiological and pathological conditions, Clin. Sci. (Lond.) 128 (2015) 181–196.
[42] Q. Wang, W. Usinger, B. Nichols, J. Gray, L. Xu, T.W. Seeley, M. Brenner, G. Guo, W. Zhang, N. Oliver, A. Lin, D. Yeowell, Cooperative interaction of CTGF and TGF-beta in animal models of fibrotic disease, Fibrogenesis Tissue Repair 4 (2011) 4.